

DOI: 10.1002/((please add manuscript number))

Article type:

**Sequential Blade Coated Acceptor and Donor Enables Simultaneous Enhancement of Efficiency, Stability and Mechanical Properties for Organic Solar Cells**

*Yilin Wang, Qinglian Zhu, Hafiz Bilal Naveed, Heng Zhao, Ke Zhou, Wei Ma\**

Y. Wang, Q. Zhu, H. B. Naveed, K. Zhou, Prof. W. Ma

State Key Laboratory for Mechanical Behavior of Materials, Xi'an Jiaotong University, Xi'an 710049,  
China

E-mail: [msewma@xjtu.edu.cn](mailto:msewma@xjtu.edu.cn),

**Abstract**

As a predominant fabrication method of organic solar cells (OSCs), casting of a BHJ structure present overwhelming advantages for achieving higher power conversion efficiency (PCE). However, long-term stability and mechanical strength are significantly crucial to realize large-area and flexible

This is the author manuscript accepted for publication and has undergone full peer review but has not been through the copyediting, typesetting, pagination and proofreading process, which may lead to differences between this version and the [Version of Record](#). Please cite this article as doi: [10.1002/aenm.201903609](https://doi.org/10.1002/aenm.201903609).

This article is protected by copyright. All rights reserved.

devices. Here, we considered controlling blend film morphology as an effective way towards co-optimizing device performance, stability and mechanical properties. We report a PCE of 12.27% for a P-i-N structured OSC processed by sequential blade casting (SBC). Our device not only outperforms the as cast BHJ devices (11.01%), but also shows impressive stability and mechanical properties. We corroborated such enhancements with improved vertical phase separation and purer phases towards more efficient transport and collection of charges. Moreover, adaptation of SBC strategy here would result in thermodynamically favorable nanostructures towards more stable film morphology, and thus improving the stability and mechanical properties of devices. Such co-optimization of OSCs would pave ways towards realizing highly efficient large area flexible devices for future endeavors.

**Keywords:** sequential blade casting, stability and mechanical properties, organic solar cells, morphology, vertical phase separation.

Solution-processed bulk heterojunction (BHJ) organic solar cells (OSCs) have attracted enormous attentions because of the high flexibility, light weight and excellent compatibility with printing and roll-to-roll processing. Impressive chemical structure design and synthesis of organic semiconducting

This article is protected by copyright. All rights reserved.

materials has pushed the power conversion efficiencies (PCE) of OSCs to 16%.<sup>[1-5]</sup> Certified PCE of BHJ devices are at the same level as commercial solar cells.<sup>[6]</sup> However, when it comes to large-scale manufacturing, these devices must show excellent reproducibility. In addition, further daily applications of solar cells demands for flexible devices. Therefore, stability and mechanical properties of OSCs has to be optimized as a priority along with the device performance towards realizing highly efficient large area devices with high reproducibility. It has been firmly established that microstructure of photoactive layer is closely associated with the efficiency as well as the stability and mechanical properties of BHJ devices. Careful morphology control can therefore provide effective pathways to co-optimize these properties of OSCs. Literature presents several contradictions in regards to achieve excellent efficiency, stability and mechanical properties. For example, increased molecular ordering could be beneficial in improving the PCE and stability of BHJ devices, but at the same time such rigid molecular network would provide possible crack points for external tension. In another scenario, larger interfacial areas in BHJ structure provides efficient charge generation towards impressive device performance, while at the same time those D/A interfaces are unstable leading fast degradation of device. D/A interfaces also provide possible crack points for external stress. Therefore, novel approaches should be explored for co-optimization of efficiency, stability and mechanical properties of OSCs through precise morphology control.

This article is protected by copyright. All rights reserved.

The task of controlling the microstructure in a single casting process is extremely complicated. BHJ structure is a combination of donor-rich, acceptor-rich, mixed amorphous or D/A domains because of the partial miscibility of the photoactive materials. As a result, undesired vertical composition profiles are often formed in the active layer during the film drying process.<sup>[7-10]</sup> Therefore, the optimization of morphological parameters and composition distribution within the BHJ often posed a serious challenge for researchers.<sup>[11-14]</sup> The optimal morphology in BHJ devices are usually a metastable state and will further move toward a thermodynamic equilibrium state to form phase separation, leading to deterioration of lifetime and performance of OSCs. Based on this view, a lot of methods are carried out to control the morphology and further enhance the performance of OSCs.<sup>[15-20]</sup> However, these approaches are generally limited to the specific materials and photovoltaic systems, therefore, it is necessary to develop a more universal and facile fabrication process to solve above problems and as well as improving the stature of OSCs.

Sequential blade coated P-i-N structure of the donor and acceptor materials can lead to a more favorable morphology and nanostructures as compared to the BHJ morphology for its promise to provide an easy and independent control over donor and acceptor phases. Additionally, P-i-N devices show less reliance on processing conditions because of the blend casting approach relies on spontaneous nanoscale phase separation to create the desired donor-acceptor network

This article is protected by copyright. All rights reserved.

morphology.<sup>[21]</sup> It is relatively easy to form the proper vertical phase separation and provide purer phases during the solution processed P-i-N devices, avoiding the difficulty of controlling the bulk morphology. In short, a P-i-N device can contribute to circumvent the existing issues in single-solvent BHJ device, and prove a good strategy for optimizing the morphology towards improved performance of OSCs. Besides, the film processing condition also has a crucial effect on the morphology of the active layer. It is demonstrated that blade-coating can change the degree of alignment in neat polymer film.<sup>[22, 23]</sup> In our previous work, we demonstrated through blade-coating to induce higher degree of molecular packing for both donor and acceptor. Blade-coating can partially replace the role of the additive 1,8-diiodooctane (DIO), realizing an optimal morphology by reducing the impact of slower morphology evolution caused by evaporation of high boiling point DIO residual.<sup>[24]</sup> Thus, blade-coating is deemed to be an efficient strategy to optimize the morphology of active layer in the process of fabricating OSCs. Furthermore, blade-coating exhibits excellent compatibility with large-area roll-to-roll coating and promising impressive reproducibility of lab-scale fabrication on large-scale manufacturing.<sup>[25-27]</sup> However, devices remain vulnerable in terms of lifetime stability and under considerable mechanical stress.

Stability of device is a critical factor for the practical application of OSCs. Morphology evolutions of active layers have verified to be responsible for device degradation.<sup>[28]</sup> By contrast, the morphology

This article is protected by copyright. All rights reserved.

of P-i-N devices is quite different from the BHJ devices due to different film forming process. In addition, incorporating macromolecule into acceptor will be benefitted to improve the long-term stability of P-i-N devices, which is mainly due to the macromolecule can inhibit molecular diffusion through formation of network fibers. Apart from the lifetime stability, the mechanical property is also an indispensable property for achieving flexible and large-area OSCs. To improve that part, photoactive film nanostructure must remain stable over considerable time and adequate crystalline donor/acceptor features to resist mechanical stress.<sup>[29]</sup> We have seen polymer/polymer blend films exhibiting excellent mechanical property for their obvious advantage of providing excellent inter-chain network, forming a large plastic zone at the crack tip during the process of applying stress. However, photovoltaic performance of all-polymer devices is limited due to large phase separation and inadequate absorption.<sup>[30-33]</sup> Encouragingly, we have shown that SBC processing method provides a suitable D/A interface area and purer phase, resulting in a more favorable nano-morphology, leading to a more stable blend film morphology towards improved mechanical property of OSCs. We propose SBC method here to improve mechanical property of polymer:non-fullerene devices. We believe that SBC may prove to be a promising strategy to co-optimize efficiency, stability and mechanical properties of OSCs.

Author Manuscript

This article is protected by copyright. All rights reserved.

In this work, we fabricated highly efficient OSCs in ambient environment via controlled nanostructures of photoactive film using SBC strategies. Based on the optimized morphology, the inverted P-i-N device with structure of ITO/ZnO/FOIC ( $x\%$  N2200)/PTB7-Th/MoO<sub>3</sub>/Ag exhibits the highest PCE of 12.27% in comparison with the optimal PCE of 11.01% for the control BHJ device (ITO/ZnO/PTB7-Th:FOIC/MoO<sub>3</sub>/Ag). Experimental results show that the gradient donor and acceptor distribution was formed during sequential deposition process. In favor of this vertical stratification, the crystallinity of FOIC was enhanced, which is beneficial to the charge transport, translating into the enhanced FF of devices. Importantly, the un-encapsulated OSCs based on SBC processing method exhibit superior stability and maintain  $\approx 90\%$  of the original PCE value after storage for 30 days, compare with about 78% of the BHJ devices. We have attributed this enhanced lifetime of device to a thermodynamically stable and vertical stratified morphology of photoactive film. Moreover, the mechanical stability of the P-i-N devices is enhanced effectively compare to the corresponding BHJ devices, due to the suitable D/A interface area and purer phase, which may provide less possibility to generate crack points within photoactive film. It is worth noting that the low-content N2200 can inhibit molecular diffusion through formation of network fibers, leading to purer phases and stable morphology, which is also beneficial in improving the lifetime and mechanical stability of P-i-N devices. Such a stable morphology presents the way forwards towards realizing highly efficient flexible OSCs with robust mechanical properties.

This article is protected by copyright. All rights reserved.

The chemical structures of PTB7-Th, FOIC and N2200 are shown in **Figure 1a**, and the corresponding UV-vis absorption spectra are present in **Figure 1b**. The PTB7-Th exhibits strong absorption between 550-750 nm and the FOIC possesses strong absorption in 650-900 nm, showing an excellent complementary light absorption. From absorption spectra, the intensity at  $\approx$ 835 nm of the film based on FOIC+N2200+DIO and FOIC+DIO enhanced slightly compared to the FOIC, indicating stronger aggregations and orderings.<sup>[34]</sup> **Figure 1c** and **Figure 1d** show the diagram of blade-coating and sequential casting. To verify whether the changes of molecular aggregation will affect the device performance, different structures of devices were fabricated. Photoactive films were fabricated in ambient environment to extending usability of our strategy to realize highly efficient devices. The current-density-voltage (*J-V*) curves are shown in **Figure 2a**, while the detailed photovoltaic characteristics are listed in **Table 1** and **Tables S1-S3**. The P-i-N device is obtained with structure of ITO/ZnO/FOIC/PTB7-Th/MoO<sub>3</sub>/Ag and offers a PCE of 11.37%. Increasing the volume ratio of FOIC and DIO from 0% to 0.3%, the  $J_{sc}$  improves from 23.89 to 24.41 mA cm<sup>-2</sup>. Impressively, by adding 3% N2200 to above-mentioned FOIC solution containing 0.3% DIO, the P-i-N device exhibited the highest PCE of 12.27% with a short circuit current density ( $J_{sc}$ ) of 24.36 mA/cm<sup>2</sup>, an open-circuit voltage ( $V_{oc}$ ) of 0.73 V, and a fill factor (FF) of 68.9%. PCE of corresponding BHJ device is limited to 11.01% mainly because of the inferior  $J_{sc}$  and FF values. Clearly, the PCE and FF values of P-i-N

This article is protected by copyright. All rights reserved.

devices are higher than those obtained in BHJ devices using the same batches of materials. The current density integrated from the EQE data are 21.67, 23.30, 23.56 and 23.23 mA cm<sup>-2</sup> for PTB7-Th:FOIC, PTB7-Th/FOIC PTB7-Th/FOIC+DIO and PTB7-Th/FOIC+N2200+DIO films based devices, respectively (**Figure 2b**). Integrated  $J_{sc}$  agrees well with those obtained from J-V characterization. To better understand why these P-i-N devices showed such high performance, the UV-vis absorption and photoluminescence (PL) spectra were used to test the features in aggregation and quenching behaviors of photoactive films. As shown in **Figure 2c**, PTB7-Th/FOIC film shows an increase in the 0-0 transition peaks and a slightly red shift in the 0-0 transition energy compared to the PTB7-Th:FOIC film. A more prominent increase in the 0-0 transition peaks are exhibited in PTB7-Th/FOIC+DIO and PTB7-Th/FOIC+N2200+DIO films, indicative of significant enhancement of molecular ordering. In addition, the P-i-N films exhibit weaker PL intensity with respect to the BHJ film, indicating inferior recombination during their rapid charge transfer. Therefore, the D/A interfacial area for P-i-N films are large enough to provide excellent exciton dissociation (**Figure 2d**).

Author Manuscript

This article is protected by copyright. All rights reserved.

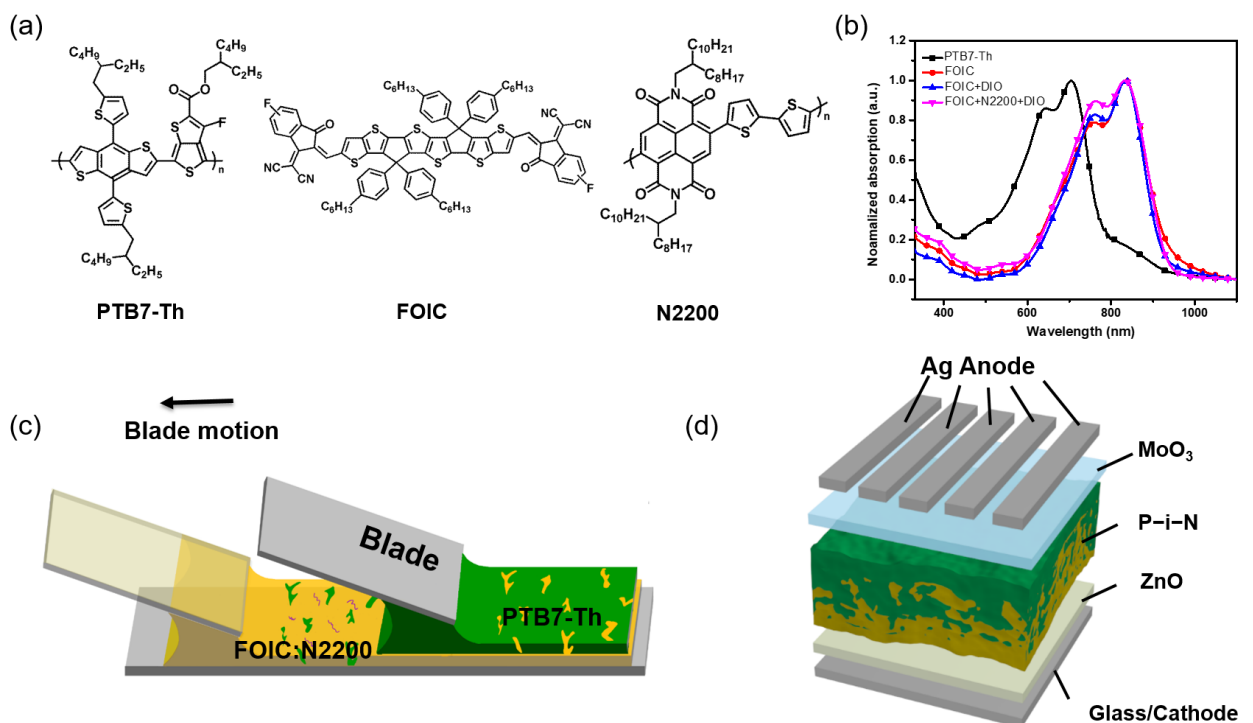


**Figure 1.** a) Chemical structures of PTB7-Th, FOIC and N2200. b) The normalized UV-vis absorption spectra of PTB7-Th, FOIC, FOIC+DIO and FOIC+DIO+N2200 films. The diagrams of c) blade-coating and d) P-i-N device structure.

**Table 1.** Detailed photovoltaic parameters of blade-coated OSCs under AM 1.5G 100 mW cm<sup>-2</sup> illumination. (Average PCEs obtained from 12 devices)

Devices	N2200 content	Additive (DIO)	$J_{sc}$ (mA/cm <sup>2</sup> )	$V_{oc}$ (V)	FF (%)	PCE (%)	Film thickness

This article is protected by copyright. All rights reserved.

						(nm)
BTU	w/o	w/o	$22.74 \pm 0.23$	$0.72 \pm 0.01$	$66.2 \pm 0.52$	$10.91 \pm 0.12(11.01)$
	w/o		$23.45 \pm 0.44$	$0.72 \pm 0.01$	$66.4 \pm 0.45$	$11.26 \pm 0.09(11.37)$
P-i-N	w/o		$24.23 \pm 0.22$	$0.72 \pm 0.01$	$67.8 \pm 0.21$	$11.83 \pm 0.15(11.99)$
	0.3%		$24.17 \pm 0.23$	$0.72 \pm 0.01$	$68.6 \pm 0.32$	$12.14 \pm 0.13(12.27)$
						50+40

Charge generation, extraction and recombination characteristics were studied to further clarify the improved photovoltaic performance. The recombination mechanisms of different device structures were studied by measuring  $V_{oc}$  at various light intensities from 10 to 100 mW/cm<sup>2</sup> (**Figure 2e**). The slope of  $V_{oc}$  versus the natural logarithm of the light intensity gives slope close to  $kT/q$ , where  $k$ ,  $T$ , and  $q$  are the Boltzmann constant, temperature in Kelvin, and the elementary charge, respectively. The fitted slopes are 1.25, 1.17, 1.12 and 1.08  $kT/q$ , for PTB7-Th:FOIC, PTB7-Th/FOIC PTB7-Th/FOIC+DIO and PTB7-Th/FOIC+N2200+DIO based devices, respectively. It confirms our earlier implication of the lowest bimolecular recombination for optimized device structure PTB7-Th/FOIC+N2200+DIO. More importantly, by incorporating 3% N2200 into FOIC, the slope is the lowest, for which we have realized the highest FF in PTB7-Th/FOIC+N2200+DIO devices. Furthermore, electron mobility ( $\mu_e$ ) and hole mobility ( $\mu_h$ ) were measured by using the space charge

limited current (SCLC) method on the basis of the Mott-Gurney equation.<sup>[35, 36]</sup> The mobility

measurements are shown in **Figure 2f** and **Figure S1** with specific values are summarized in **Table S4**.

Notably, the P-i-N device exhibit higher  $\mu_e$  than that of the BHJ device, mainly attributed to the

improvement of acceptor crystallization. It is worth noting that the hole mobility and electron

mobility of the PTB7-Th/FOIC+N2200+DIO based device are estimated to be  $2.46 \times 10^{-4}$  and  $2.71 \times 10^{-4}$

$\text{cm}^2 \text{ V}^{-1} \text{ s}^{-1}$ , respectively, exhibiting a most balanced mobility with the  $\mu_e/\mu_h$  of 0.907, which would

contribute to a high FF of 68.9%. These results confirm that the crystallinity of FOIC was enhanced by

using SBC processing method, probably because a gradient donor and acceptor distribution was

formed, which is benefited to reduce the bimolecular recombination, and hence improve

photovoltaic performance.

Author Manuscript

This article is protected by copyright. All rights reserved.

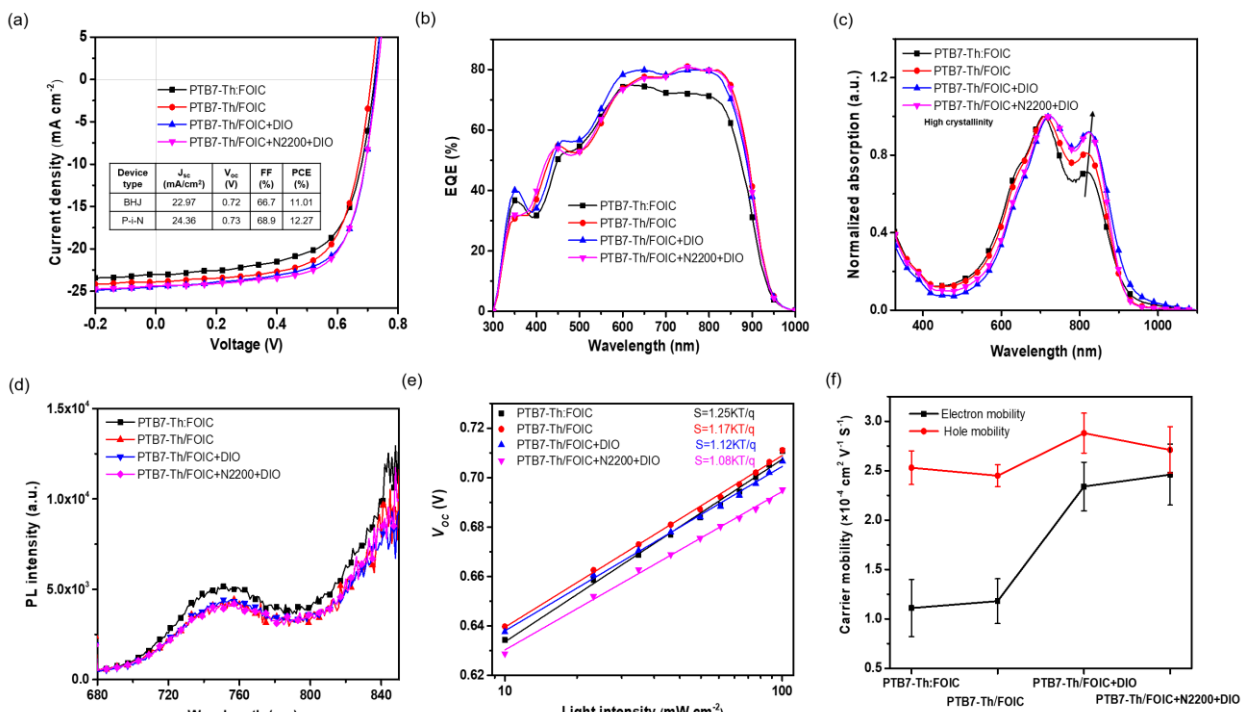


**Figure 2.** a)  $J-V$  curves of BHJ device and P-i-N devices. b) EQE curves. c) The normalized UV-vis absorption spectra of BHJ and P-i-N structure films. d) PL spectra e) dependence of open-circuit voltage on light intensity and f) the carrier mobility of BHJ and P-i-N devices.

In addition, we can speculate for an enhanced crystallinity of FOIC domains with its increased purity of phases at the bottom part of the film. In order to better understand morphology characteristics, grazing incident wide-angle X-ray scattering (GIWAXS)<sup>[37]</sup> measurement was adopted to provide the information of molecular ordering and crystallization orientation. The 2D GIWAXS patterns and

corresponding line profiles are depicted in **Figure 3** **Figure S2** and **Figure S3**. The crystallization coherence length (CCL) was quantified using Scherrer equation.<sup>[36, 38, 39]</sup> The pure FOIC film exhibit highly ordered lamellar stacking (100) peak at low  $q$  ( $q=0.45 \text{ \AA}^{-1}$ ) in in-plane direction. The scattering peaks of P1-N films get much stronger and sharper than those of the BHJ films, indicating a higher degree of molecular ordering for these films. Increasing DIO content from 0% to 0.3% has seen further enhancement of FOIC crystallinity as confirmed by increased quantified CCL from 18.2 to 22.7 nm. After incorporation 3% N2200 in FOIC, the calculated CCL value was increased to 23.4 nm, confirming the stronger crystallization propensity of the FOIC (**Table S5**). Similar variations have also been observed by fitting the  $\pi-\pi$  stacking peaks (010) for FOIC. Notably, PTB7-Th/FOIC+10%N2200+DIO exhibited the highest CL of (100) and (010) for FOIC, mainly because of poor miscibility between FOIC and N2200. According to the Flory-Huggins model, the interaction parameters ( $\chi$ ) are calculated to be 1.16 for  $\chi_{\text{FOIC, N2200}}$ , (**Figure S4** and **Table S6**) suggesting that poor miscibility and weaker interaction with between FOIC and N2200, offering very little barrier for FOIC to form crystalline phases.<sup>[40]</sup> And we consider that the highest crystallinity of FOIC in PTB7-Th/FOIC+10%N2200+DIO film is also resulted in the film-drying rate. By adding 10%N2200, the film-drying rate become slower compared with other films, which would prompt FOIC crystal nucleuses grow bigger, leading to higher relative degree of crystallinity.<sup>[41]</sup> (**Figure S5**). As expected, the increased crystallization of FOIC mainly due to the formation of the more desired vertical phase

This article is protected by copyright. All rights reserved.

distribution, leading to a purer phases of FOIC, which is in good agreement with the thickness dependent vertical phase distribution analysis. SBC processed OSCs has proved to be an efficient strategy to optimize the vertical phase distribution, testing by the film-depth-dependent light absorption<sup>[42]</sup> (**Figure S6b**). Furthermore, we analyzed the orientation distribution of the (100) peak, the polar angle,  $\omega$ , is defined as the angle between the scattering vector and the substrate normal. The scattering intensity near  $\omega = 90^\circ$  and  $0^\circ$  are associated with face-on ( $A_{xy}$ ) and edge-on ( $A_z$ ) orientations relative to the substrate, respectively. The value of  $A_{xy}/A_z$  is a measurement of face-on contribution, defined as the ratio between the integrated area ( $A_{xy}$ ) where  $45^\circ < \omega < 90^\circ$  and the area ( $A_z$ ) where  $0^\circ < \omega < 45^\circ$ .<sup>[43]</sup> The calculated  $A_{xy}/A_z$  ratio of PTB7-Th:FOIC, PTB7-Th/FOIC PTB7-Th/FOIC+DIO and PTB7-Th/FOIC+N2200+DIO films are 1.02, 1.14, 1.24 and 1.25, respectively. The increased population of face-on crystallites further confirms efficient charge transfer and transport pathways towards improved  $J_{sc}$  and FF values.

# Author Manuscript

This article is protected by copyright. All rights reserved.

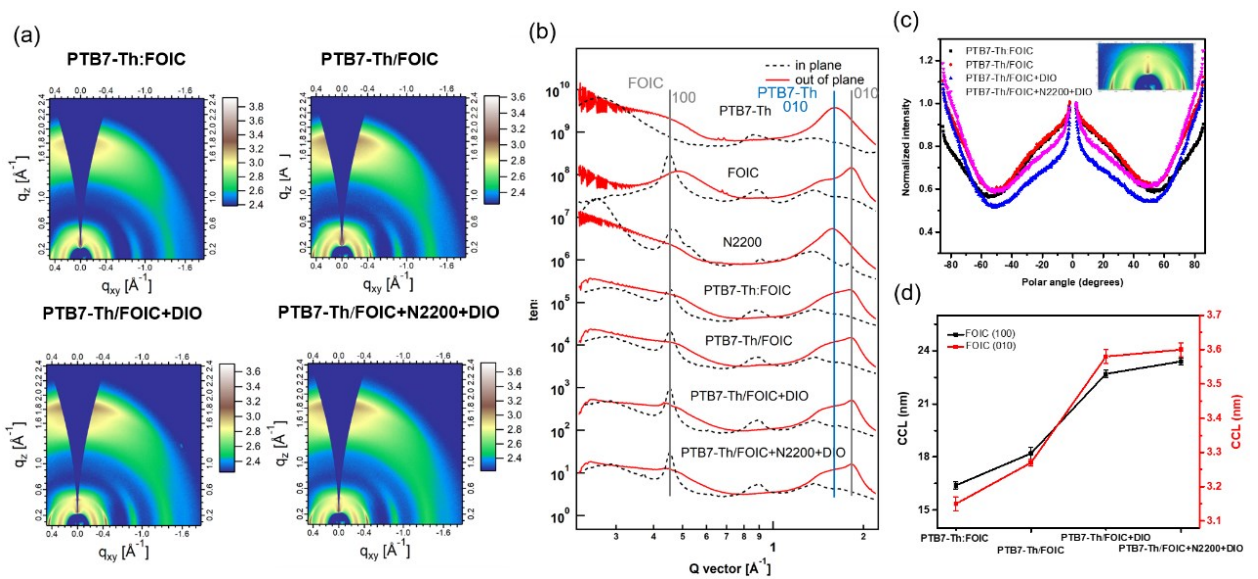


**Figure 3.** a) GIWAXS 2D scattering patterns b) line profiles c) pole figure of (100) diffraction peak d)

the calculated CCL values of (010) and (100) peak of PTB7-Th:FOIC, PTB7-Th/FOIC, PTB7-Th/FOIC+DIO and PTB7-Th/FOIC+N2200+DIO films.

Morphology degradation of active layer have proved to be responsible for device degradation, for example, improved molecular ordering and optimized D/A interfaces would inhibit the diffusion of adjacent molecules, to improve the stability of device.<sup>[44]</sup> According to **Figure 4a**, un-encapsulated OSCs based on P-i-N devices without DIO exhibit superior stability and maintain  $\approx 90\%$  of the original PCE value after storage for 30 days compared to  $\approx 78\%$  of the control BHJ devices. The experiment result shows that SBC processing method provides more favorable phase separation with purer

**WILEY-VCH**

phases, (**Figure S7-S8 , Table S7**) which is in thermodynamically stable state and promised towards realizing superior stability of OSCs. It is worth noting that dissociation of residual DIO would destroy morphology of active layer, leading to the degradation of PCE. However, by incorporating low-content N2200 into FOIC, the long-term stability of the P-i-N device has increased. This is mainly due to ability of fibril N2200 network inhibiting the molecular diffusion and resulting in stable blend film nanostructures. Therefore, in order to obtain stable morphology and device performance, interfacial structure and phase separation should be carefully controlled. More importantly, mechanical property of the devices is an indispensable factor for achieving flexible and wearable OSCs.<sup>[45]</sup> For example, OSCs used as wearable electronics should be able to withstand tensile strain of at least 20-30%.<sup>[46]</sup> Several reviews have been published on the development of mechanical property of OSCs, indicating that acceptor type, length of the alkyl side-chain of polymer, polymer molecular weight and additive will have a effect on the mechanical property of the device, which provide guidelines for the co-optimization of both mechanical and photovoltaic properties.<sup>[46-52]</sup> (The molecular weight information of PTB7-Th and N2200 is shown in the Figure S9) Additionally, the mechanical property of the devices is also closely related to the morphology parameters, such as D/A interfaces and molecular order.<sup>[29, 53]</sup> The tensile parameters were measured to acquire a quantitative comparison of the mechanical property. The thickness of all the films were maintained at around 90-100 nm (for P-i-N devices, the thickness of FOIC:PTB7-Th≈1:1) because of the

This article is protected by copyright. All rights reserved.

mechanical properties of thin films are a strong function of film preparation condition, such as film thickness. The representative stress-strain curves (**Figure 4b**) show dramatically different fracture behaviors of BHJ film and P-i-N films under optimized device conditions. The BHJ film shows no obvious plastic deformation region and breaks at a short elongation, while the P-i-N films exhibited a wide deformation and crack at a much longer elongation, the crack-onset strain (COS) are 3.1%, 11.5%, 12.4% and 18.5% for PTB7-Th:FOIC, PTB7-Th/FOIC PTB7-Th/FOIC+DIO and PTB7-Th/FOIC+N2200+DIO based films. Surprisingly, the COS of PTB7-Th/FOIC films is 6-fold higher compared with that of PTB7-Th:FOIC film, announcing a stretchable film which is favorable in fabricating flexible OSCs through sequential deposition. Additionally, the DIO incorporating in the films induces fine nanomorphology and increase the crystallinity of FOIC, which increases the stiffness and strength and reduces the ductility of the films, resulted in a decrease of COS. By incorporating N2200 in FOIC, the flexible polymer bridging chains of N2200 provide an interaction between polymer-rich and small molecule-rich domains, resulting in enhanced mechanical strength. Regarded to why the P-i-N structure could improve the mechanical property compared with the BHJ, we attributed to the proper D/A interfaces and purer phases. As we all know, small molecule have the intrinsic characteristic of stiffness and brittleness, like PCBM, which is the performance limiting component,<sup>[47]</sup> possible crack points usually occur at the interfacial while provide for external stress. Therefore, The proper D/A interfaces and purer phases in P-i-N films exhibit excellent mechanical

This article is protected by copyright. All rights reserved.

resilience. We propose that optimizing D/A interfaces carefully with bulk phases would provide least crack points, leading to a stronger elongation. Such excellent properties are desired for realizing photovoltaic performance and large-area roll-to-roll processing of OSCs. Through **Figure 4**, we have illustrated summary of our efforts in co-optimizing efficiency, stability and mechanical properties of polymer:non-fullerene based control BHJ (PTB7-Th:FOIC) to SBC P-i-N structured (PTB7-Th/FOIC+N2200+DIO) OSCs.

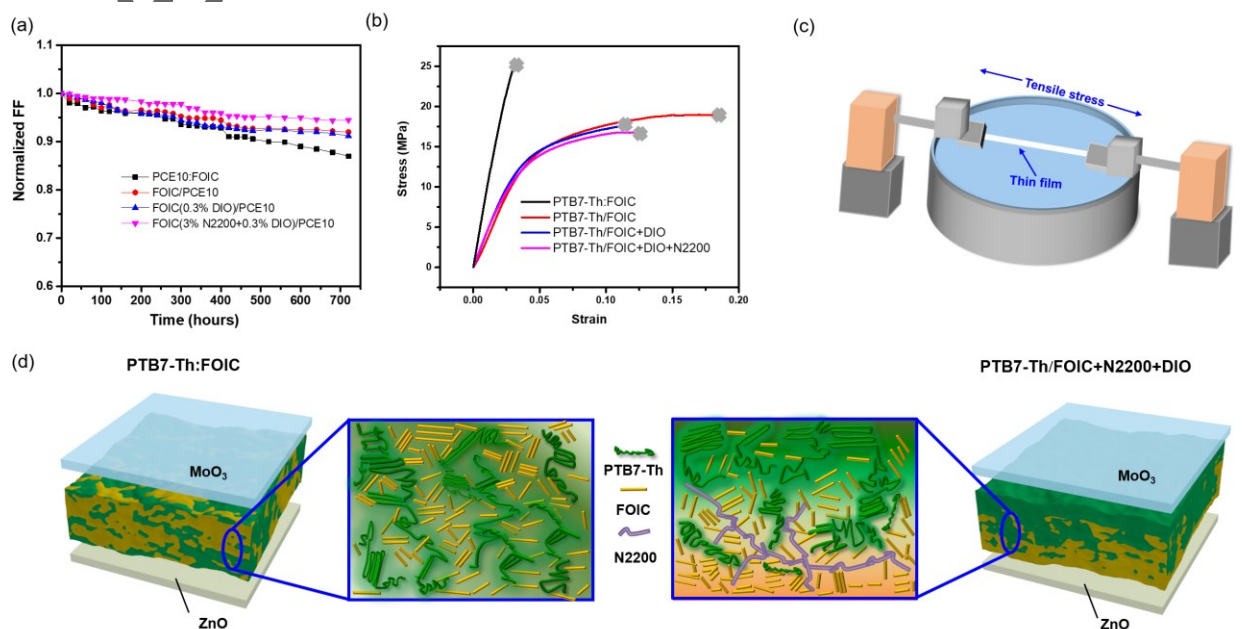


**Figure 4.** a) Normalized PCE of PTB7-Th:FOIC, PTB7-Th/FOIC, PTB7-Th FOIC+DIO/and /PTB7-Th/FOIC+N2200+DIO devices as a function of time in nitrogen atmosphere. b) Stress-strain curves of PTB7-Th:FOIC, PTB7-Th/FOIC, PTB7-Th/FOIC+DIO and PTB7-Th/FOIC+N2200+DIO films. c)

Schematic illustration of tensile tester setup for floated ultrathin film. d) Schematic diagram of morphology of PTB7-Th:FOIC and PTB7-Th/FOIC+N2200+DIO films.

In this work, we have devised a way forward to co-optimize photovoltaic parameters with stability and mechanical properties of OSCs. Using sequential blade casting (SBC) method, a highly efficient (12.27%) non-fullerene OSCs was fabricated in ambient environment, which is higher than its corresponding BHJ control device (11.01%). Significantly different morphology of P-i-N from BHJ film, as we controlled the vertical phase separation and purity of acceptor phases to drive the improved charge transport and collection processes towards highly efficient OSCs. Moreover, we have shown that SBC processing method provide a suitable D/A interface area to go with purer phases, which resulted in thermodynamically stable nanostructures leading a more favorable blend film morphology towards improved stability and mechanical properties of OSCs. It is worth noting that the low-content N2200 can inhibit molecular diffusion by forming a fibril network, which is also beneficial in improving the stability and mechanical properties of P-i-N devices. Our results offer a simple pathway towards realizing highly efficient OSCs with improved stability and mechanical properties for their practical applications.

#### Acknowledgements

This article is protected by copyright. All rights reserved.

Y. Wang and Q. Zhu contributed equally. Thanks for the support from Ministry of science and technology (No. 2016YFA0200700), NSFC (21704082, 21875182, 21534003, 51320105014), China Postdoctoral Science Foundation (2017M623162). X-ray data was acquired at beamlines 7.3.3 and 11.0.1.2 at the Advanced Light Source, which is supported by the Director, Office of Science, Office of Basic Energy Sciences, of the U.S. Department of Energy under Contract No. DE-AC02-05CH11231. The authors thank Chenhui Zhu at beamline 7.3.3, and Cheng Wang at beamline 11.0.1.2 for assistance with data acquisition. The authors thank prof. Xugang Guo and Dr. Kui Feng at the Materials Characterization and Preparation Center, Southern University of Science and Technology for assistance with the acquisition of molecular weight information.

#### Supporting Information

Supporting Information is available from the Wiley Online Library or from the author.

Received: ((will be filled in by the editorial staff))

Revised: ((will be filled in by the editorial staff))

Published online: ((will be filled in by the editorial staff))

This article is protected by copyright. All rights reserved.

## References

- [1] J. Yuan, Y. Zhang, L. Zhou, G. Zhang, H.-L. Yip, T.-K. Lau, X. Lu, C. Zhu, H. Peng, P. A. Johnson, M. Leclerc, Y. Cao, J. Ulanski, Y. Li, Y. Zou, *Joule* **2019**, *3*, 1140.
- [2] Q. An, X. Ma, J. Gao, F. Zhang, *Sci. Bull.* **2019**, *64*, 504.
- [3] B. Fan, D. Zhang, M. Li, W. Zhong, Z. Zeng, L. Ying, F. Huang, Y. Cao, *Sci. China Chem.* **2019**, *62*, 746.
- [4] M.-A. Pan, T.-K. Lau, Y. Tang, Y.-C. Wu, T. Liu, K. Li, M.-C. Chen, X. Lu, W. Ma, C. Zhan, *J. Mater. Chem. A* **2019**, *7*, 20713.
- [5] T. Yan, W. Song, J. Huang, R. Peng, L. Huang, Z. Ge, *Adv. Mater.* **2019**, *31*, 1902210.
- [6] S. Li, L. Ye, W. Zhao, H. Yan, B. Yang, D. Liu, W. Li, H. Ade, J. Hou, *J. Am. Chem. Soc.* **2018**, *140*, 7159.
- [7] Y. Yan, X. Liu, T. Wang, *Adv. Mater.* **2017**, *29*, 1601674.
- [8] J. Min, N. S. Güldal, J. Guo, C. Fang, X. Jiao, H. Hu, T. Heumüller, H. Ade, C. J. Brabec, *J. Mater. Chem. A* **2017**, *5*, 18101.
- [9] J. Chen, Z. Bi, X. Xu, Q. Zhang, S. Yang, S. Guo, H. Yan, W. You, W. Ma, *Adv. Sci.* **2019**, *6*, 1801560.
- [10] L. Huang, G. Wang, W. Zhou, B. Fu, X. Cheng, L. Zhang, Z. Yuan, S. Xiong, L. Zhang, Y. Xie, A. Zhang, Y. Zhang, W. Ma, W. Li, Y. Zhou, E. Reichmanis, Y. Chen, *ACS Nano* **2018**, *12*, 4440.
- [11] C. J. Brabec, M. Heeney, I. McCulloch, J. Nelson, *Chem. Soc. Rev.* **2011**, *40*, 1185.
- [12] Z. Xiao, Y. Yuan, B. Yang, J. VanDerslice, J. Chen, O. Dyck, G. Duscher, J. Huang, *Adv. Mater.* **2014**, *26*, 3068.
- [13] L. Ye, H. Hu, M. Ghasemi, T. Wang, B. A. Collins, J.-H. Kim, K. Jiang, J. H. Carpenter, H. Li, Z. Li, T. McAfee, J. Zhao, X. Chen, J. L. Y. Lai, T. Ma, J.-L. Bredas, H. Yan, H. Ade, *Nat. Mater.* **2018**, *17*, 253.

This article is protected by copyright. All rights reserved.

- [14] S. Kouijzer, J. J. Michels, M. van den Berg, V. S. Gevaerts, M. Turbiez, M. M. Wienk, R. A. Janssen, *J. Am. Chem. Soc.* **2013**, *135*, 12057.
- [15] R. Yu, H. Yao, L. Hong, Y. Qin, J. Zhu, Y. Cui, S. Li, J. Hou, *Nat. Commun.* **2018**, *9*, 4645.
- [16] P. Cheng, C. Yan, T. K. Lau, J. Mai, X. Lu, X. Zhan, *Adv. Mater.* **2016**, *28*, 5822.
- [17] P. Cheng, C. Yan, Y. Wu, J. Wang, M. Qin, Q. An, J. Cao, L. Huo, F. Zhang, L. Ding, Y. Sun, W. Ma, X. Zhan, *Adv. Mater.* **2016**, *28*, 8021.
- [18] Z. Li, F. Wu, H. Lv, D. Yang, Z. Chen, X. Zhao, X. Yang, *Adv. Mater.* **2015**, *27*, 6999.
- [19] X. Du, T. Heumueller, W. Gruber, A. Classen, T. Unruh, N. Li, C. J. Brabec, *Joule* **2019**, *3*, 215.
- [20] H. Cha, J. Wu, A. Wadsworth, J. Nagitta, S. Limbu, S. Pont, Z. Li, J. Searle, M. F. Wyatt, D. Baran, J. S. Kim, I. McCulloch, J. R. Durrant, *Adv. Mater.* **2017**, *29*, 1701156.
- [21] F. Liu, C. Wang, J. K. Baral, L. Zhang, J. J. Watkins, A. L. Briseno, T. P. Russell, *J. Am. Chem. Soc.* **2013**, *135*, 19248.
- [22] L. Shaw, P. Hayoz, Y. Diao, J. A. Reinschach, J. W. To, M. F. Toney, R. T. Weitz, Z. Bao, *ACS Appl. Mater. Interfaces* **2016**, *8*, 9285.
- [23] W. Ma, J. Reinschach, Y. Zhou, Y. Diao, T. McAfee, S. C. B. Mannsfeld, Z. Bao, H. Ade, *Adv. Funct. Mater.* **2015**, *25*, 3131.
- [24] X. Liao, L. Zhang, X. Hu, L. Chen, W. Ma, Y. Chen, *Nano Energy* **2017**, *41*, 27.
- [25] H. W. Ro, J. M. Downing, S. Engmann, A. A. Herzing, D. M. DeLongchamp, L. J. Richter, S. Mukherjee, H. Ade, M. Abdelsamie, L. K. Jagadamma, *Energy Environ. Sci.* **2016**, *9*, 2835.
- [26] Q. Kang, L. Ye, B. Xu, C. An, S. J. Stuard, S. Zhang, H. Yao, H. Ade, J. Hou, *Joule* **2019**, *3*, 227.
- [27] L. H. Rossander, H. F. Dam, J. E. Carlé, M. Helgesen, I. Rajkovic, M. Corazza, F. C. Krebs, J. W. Andreasen, *Energy Environ. Sci.* **2017**, *10*, 2411.
- [28] A. Guerrero, G. Garcia-Belmonte, *Nanomicro Lett.* **2017**, *9*, 10.
- [29] K. Zhou, J. Xin, W. Ma, *ACS Energy Letters* **2019**, *4*, 447.

This article is protected by copyright. All rights reserved.

- [30] E. Zhou, J. Cong, K. Hashimoto, K. Tajima, *Adv. Mater.* **2013**, *25*, 6991.
- [31] D. Mori, H. Benten, I. Okada, H. Ohkita, S. Ito, *Energy Environ. Sci.* **2014**, *7*, 2939.
- [32] H. Kang, M. A. Uddin, C. Lee, K. H. Kim, T. L. Nguyen, W. Lee, Y. Li, C. Wang, H. Y. Woo, B. J. Kim, *J. Am. Chem. Soc.* **2015**, *137*, 2359.
- [33] Z. Li, X. Xu, W. Zhang, X. Meng, W. Ma, A. Yartsev, O. Inganas, M. R. Andersson, R. A. Janssen, E. Wang, *J. Am. Chem. Soc.* **2016**, *138*, 10935.
- [34] Y. Liu, J. Zhao, Z. Li, C. Mu, W. Ma, H. Hu, K. Jiang, H. Lin, H. Ade, H. Yan, *Nat. Commun.* **2014**, *5*, 5293.
- [35] S. Chen, Y. Liu, L. Zhang, P. C. Y. Chow, Z. Wang, G. Zhang, W. Ma, H. Yan, *J. Am. Chem. Soc.* **2017**, *139*, 6298.
- [36] J. Xiao, Z. Chen, G. Zhang, Q.-Y. Li, Q. Yin, X.-F. Jiang, F. Huang, Y.-X. Xu, H.-L. Yip, Y. Cao, *J. Mater. Chem. C* **2018**, *6*, 4457.
- [37] A. Hexemer, W. Bras, J. Glossinger, E. Schaible, E. Gann, R. Kirian, A. MacDowell, M. Church, B. Rude, H. Padmore, *J. Phys.: Conf. Ser.* **2010**, *247*, 012007.
- [38] D. M. Smilgies, *J. Appl. Crystallogr.* **2013**, *46*, 286.
- [39] D. M. Smilgies, *J. Appl. Crystallogr.* **2009**, *42*, 1030.
- [40] J. Xin, X. Meng, X. Xu, Q. Zhu, H. B. Naveed, W. Ma, *Matter* **2019**, *1*, 1316.
- [41] X. Gu, J. Reinschbach, B. J. Worfolk, Y. Diao, Y. Zhou, H. Yan, K. Gu, S. Mannsfeld, M. F. Toney, Z. Bao, *ACS Appl. Mater. Interfaces* **2016**, *8*, 1687.
- [42] P. Bi, T. Xiao, X. Yang, M. Niu, Z. Wen, K. Zhang, W. Qin, S. K. So, G. Lu, X. Hao, H. Liu, *Nano Energy* **2018**, *46*, 81.
- [43] A. L. Ayzner, J. Mei, A. Appleton, D. DeLongchamp, A. Nardes, S. Benight, N. Kopidakis, M. F. Toney, Z. Bao, *ACS Appl. Mater. Interfaces* **2015**, *7*, 28035.
- [44] K. C. Lee, N. G. An, S. M. Lee, J. Heo, D. S. Kim, J. Y. Kim, C. Yang, *Solar RRL* **2018**, *2*, 1700235.

This article is protected by copyright. All rights reserved.

- [45] L. V. Kayser, D. J. Lipomi, *Adv. Mater.* **2019**, *31*, 1806133.
- [46] J. Choi, W. Kim, S. Kim, T.-S. Kim, B. J. Kim, *Chem. Mater.* **2019**, *31*, 9057.
- [47] T. Kim, J.-H. Kim, T. E. Kang, C. Lee, H. Kang, M. Shin, C. Wang, B. Ma, U. Jeong, T.-S. Kim, B. J. Kim, *Nat. Commun.* **2015**, *6*, 8547.
- [48] W. Kim, J. Choi, J.-H. Kim, T. Kim, C. Lee, S. Lee, M. Kim, B. J. Kim, T.-S. Kim, *Chem. Mater.* **2018**, *30*, 2102.
- [49] S. Savagatrup, A. S. Makaram, D. J. Burke, D. J. Lipomi, *Adv. Funct. Mater.* **2014**, *24*, 1169.
- [50] J.-H. Kim, J. Noh, H. Choi, J.-Y. Lee, T.-S. Kim, *Chem. Mater.* **2017**, *29*, 3954.
- [51] J. Jung, W. Lee, C. Lee, H. Ahn, B. J. Kim, *Adv. Energy Mater.* **2016**, *6*, 1600504.
- [52] C. Lee, S. Lee, G. U. Kim, W. Lee, B. J. Kim, *Chem. Rev.* **2019**, *119*, 8028.
- [53] O. Awartani, B. I. Lemanski, H. W. Ro, L. J. Richter, D. M. DeLongchamp, B. T. O'Connor, *Adv. Energy Mater.* **2013**, *3*, 399.

Author Manuscript

This article is protected by copyright. All rights reserved.

WILEY-VCH

The table of contents entry

A proper vertical phase separation and purer phases of donor and acceptor is finely controlled by sequential blade casting strategy in the PTB7-Th:FOIC based organic solar cell, resulting in simultaneous enhancement of efficiency, stability and mechanical properties.

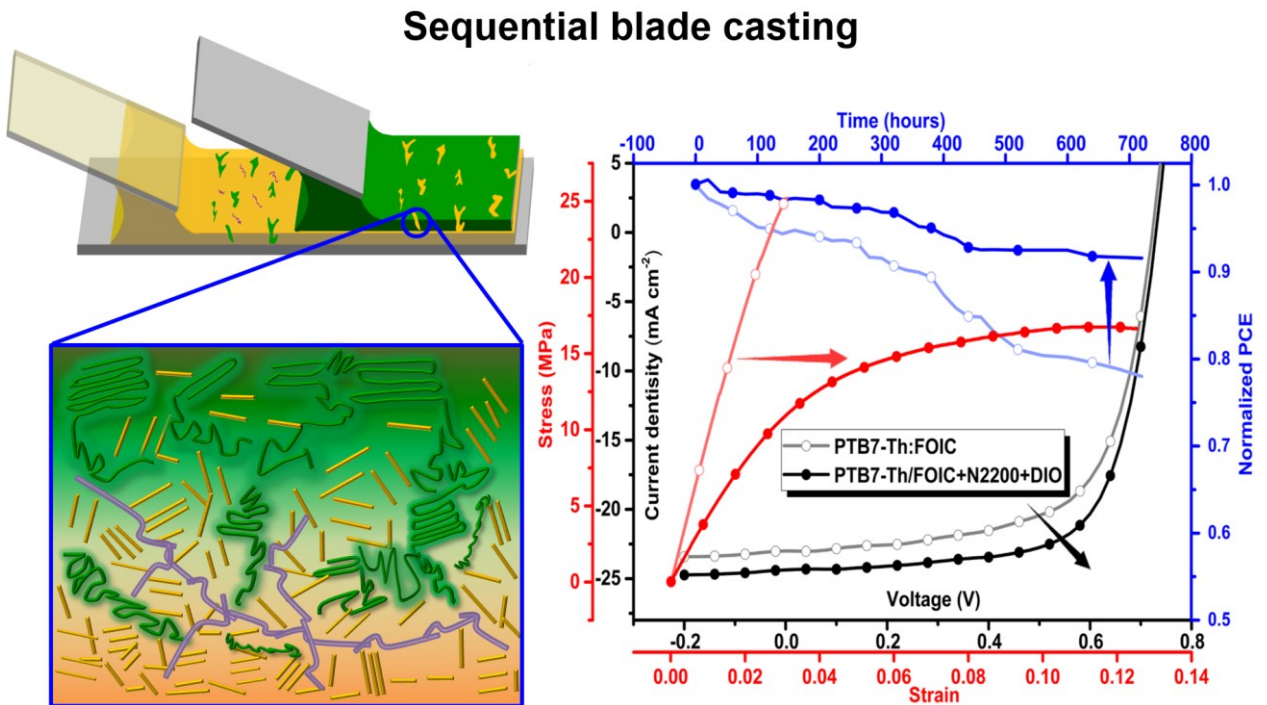
**Keywords:** sequential blade casting, stability and mechanical properties, organic solar cells, morphology, vertical phase separation

**Sequential Blade Coated Acceptor and Donor Enables Simultaneous Enhancement of Efficiency, Stability and Mechanical Properties for Organic Solar Cells**

*Yilin Wang, Qinglian Zhu, Hafiz Bilal Naveed, Heng Zhao, Ke Zhou, Wei Ma\**

This article is protected by copyright. All rights reserved.

WILEY-VCH



Author War

This article is protected by copyright. All rights reserved.